An Overview of Important Microstructural Distributions for Polyolefin Analysis

João B.P. Soares

Summary: Polyolefins with complex microstructures are becoming increasingly common in academic and industrial applications. Polyolefin analytical techniques are evolving to provide a more detailed picture of these microstructures, with the development and improvement of hyphenated-techniques and cross-fractionation methods. These modern analytical techniques provide a wealth of information on polyolefin microstructure and, despite being extremely useful, they can also be hard to interpret without the help of mathematical models that link polymerization kinetics to chain microstructure and polymer characterization results. In this paper we review some of the most important distributions for polyolefin microstructure and derive a few new expressions that help understand the results obtained with several polyolefin characterization techniques.

Keywords: polyethylene; polymer characterization; polymer fractionation; polymer microstructure; polyolefins

Introduction

The remarkable versatility of polyolefins come from the fact that ethylene, propylene and α-olefins can be copolymerized to create polymer chains with microstructures that lead to very different physical properties.

Polyolefin properties are ultimately defined by the way the monomers are connected to form linear and branched polymer chains with different degrees of regularity. It is, therefore, very important to characterize the microstructure of polyolefins and to quantify this microstructure using fundamental models.

In this short overview, we will present some important equations that describe polyolefin microstructure and discuss some modeling principles that can be used to help understand the results obtained with several polyolefin characterization techniques.

Department of Chemical Engineering, University of Waterloo, Waterloo, Ontario, Canada N2L 3G1
E-mail: jsoares@uwaterloo.ca

Distribution of Chain Length, Chemical Composition, and Long Chain Branching

The most general distribution for the microstructure of polyolefins made with coordination catalysts is given by the equation:[1,2]

$$w(r,F,i) = \frac{1}{(2i+1)!} r^{2i+1} \tau^{2i+2} \exp(-r\tau) \sqrt{\frac{r}{2\pi\beta}} \exp\left[-\frac{r(F-\overline{F})^2}{2\beta}\right] \quad (1)$$

In Equation (1), $w(r,F,i)$ is the height of the weight distribution for chains of length r, comonomer fraction F, and i long chain branches (LCB) per chain. This equation has only two parameters, β and τ, defined as:

$$\beta = \frac{}{\overline{F}(1-\overline{F})\sqrt{1-4\overline{F}(1-\overline{F})(1-r_1 r_2)}} \quad (2)$$

$$\tau = \frac{rate\ of\ transfer + rate\ of\ LCB\ formation}{rate\ of\ propagation} \quad (3)$$

Finally, $\overline{F}$ is the average fraction of comonomer in the copolymer (as calculated

from Mayo-Lewis equation, for instance) and r_1 and r_2 are the comonomer reactivity ratios.

This equation was derived based on the mechanism widely accepted for olefin polymerization with coordination catalysts where chains can propagate by monomer insertion, terminate through several transfer mechanism, and LCBs are formed by the incorporation of vinyl-terminated polymer chains, commonly called macromonomers. No other assumption were needed for model development.[1,2]

It is interesting to point out that Equation (1) becomes Stockmayer distribution for linear chains, that is, for $i = 0$:[3]

$$w(r,F) = r\tau^2 \exp(-r\tau)\sqrt{\frac{r}{2\pi\beta}}\exp\left[-\frac{r(F-\overline{F})^2}{2\beta}\right] \quad (4)$$

In addition, if we integrate Equation (4) over all comonomer compositions we obtain Flory's most probable chain length distribution (CLD):[4,5]

$$w(r) = \int_{-\infty}^{\infty} w(r,F)\mathrm{d}(F-\overline{F}) = r\tau^2\exp(-r\tau) \quad (5)$$

For linear chains, the parameter τ is the reciprocal of the number average chain length, r_n:

$$\tau = \frac{rate\ of\ transfer}{rate\ of\ propagation} = \frac{1}{r_n} \quad (6)$$

Therefore, in the same way that Stockmayer's distribution is the extension of Flory's distribution to binary copolymers, Equation (1) is the extension of Stockmayer's distribution to non-linear copolymers. We will now start applying Equation (1), (4), and (5) to several common polyolefin characterization techniques.

Molecular Weight Distribution of Linear Chains

Molecular weight distributions (MWD) of polyolefins made with single site catalysts follow Flory's most probable distribution, Equation (5). MWDs are usually measured with high-temperature gel permeation chromatography (GPC) and expressed in log scale. Before we can use Equation (5) to describe the experimental MWD of polyolefins, we need to apply two simple mathematical transformations. First, we need to change the CLD into a MWD using the relation,

$$w(MW)\mathrm{d}MW = w(r)\mathrm{d}r \quad (7)$$

where MW is the polymer molecular weight. Since $\mathrm{d}MW/\mathrm{d}r$ equals the molar mass of the repeating unit in the polymer chain (mw), Equation (5) becomes,

$$w(MW) = MW\hat{\tau}^2\exp(-MW\hat{\tau}) \quad (8)$$

where,

$$\hat{\tau} = \frac{\tau}{mw} = \frac{1}{r_n \cdot mw} = \frac{1}{M_n} \quad (9)$$

and M_n is the number average molecular weight of the polymer.

Equation (8) must now be rendered in log scale through the transformation:

$$w(\log MW)\mathrm{d}\log MW = w(MW)\mathrm{d}MW \quad (10)$$

Consequently:

$$w(\log MW) = 2.3026 \times MW^2\hat{\tau}^2\exp(-MW\hat{\tau}) \quad (11)$$

Figure 1 shows that the MWD of a polyethylene sample made with two metallocene catalysts supported on the same silica carrier is well represented by the superposition of two Flory's distributions. Since we have two single-site catalysts in Figure 1, the MWD of the combined polymer, $W(\log MW)$ is described by the weighed sum of two Flory's distributions,

$$W(\log MW) = m_{Zr}w(\log MW)_{Zr} + (1-m_{Zr})w(\log MW)_{Hf} \quad (12)$$

where m_{Zr} is the mass fraction of polyethylene produced by the zirconium catalyst.

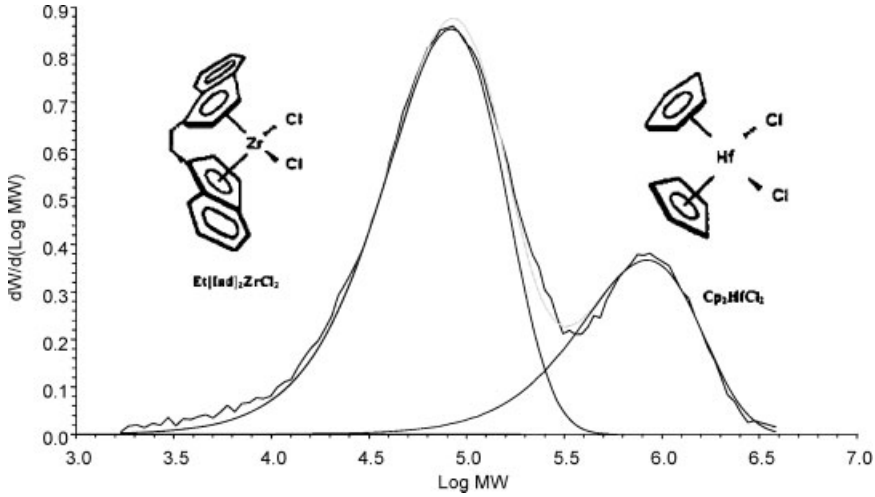

Figure 1.
Comparison of the GPC-measured MWD of a polyethylene sample made with two metallocenes supported on silica and model prediction using Flory's distribution. The peaks for polymer made with both metallocenes are described with Equation (8).[6]

This modeling concept is commonly extended to catalysts that have more than one site type, such as heterogeneous Ziegler-Natta and Phillips catalysts.[7] Figure 2 shows an example of such a MWD representation for the case of a polyethylene resin made with a heterogeneous Ziegler-Natta catalyst.

Therefore, we can generalize Equation (12) for the case of a catalyst with n

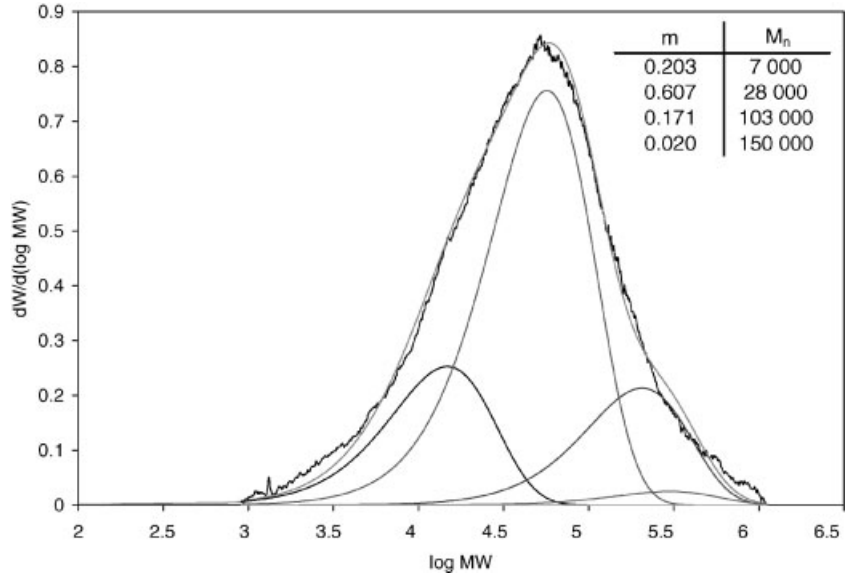

Figure 2.
MWD of a polyethylene sample made with a heterogeneous Ziegler-Natta catalyst. The MWD is represented as a superposition of four Flory's distributions, having the mass fractions (m) and number average molecular weights (M_n) indicated in the table.

different site types:

$$W(\log MW) = \sum_{j=1}^{n} m_j w_j(\log MW)$$

$$= 2.3056 \times MW^2 \sum_{j=1}^{n} m_j \hat{\tau}_j^2 \exp(-MW\hat{\tau}_j) \qquad (13)$$

Equation (13) is a statement of our first modeling principle:

Principle 1: The microstructural distribution of a polymer made with a multiple-site catalyst can be represented as a weighted superposition of distributions for single-site catalysts.

This principle must be used with care: we must keep in mind that it only provides a convenient way to represent microstructural distributions of polymers made with multiple site catalysts.

Hyphenated Techniques: GPC-IR

The use of a infrared detector (IR) with GPC is becoming increasingly popular for polyolefin characterization. This relatively simple combination permits the detection of the average chemical composition (generally reported as molar fraction of α-olefin or short chain branching frequency) as a function of molecular weight. Figure 3 shows the GPC-IR plot for a linear low density polyethylene (LLDPE) resin. We immediately notice the fingerprint mark of a heterogeneous Ziegler-Natta catalyst: as the molecular weight increases, the fraction of 1-butene in the sample decreases.

It is possible to use Modeling Principle 1 to interpret this profile. Figure 4 shows that the MWD can be represented as a superposition of five Flory's distributions. If we assume that each distribution is associated with an active site type that produces LLDPE with a distinct average molar fraction of 1-butene (F_j), we can say that the overall 1-butene fraction measured by the IR detector in a given molecular weight (ΔMW) interval is,

$$F(\Delta MW) = \sum_{j=1}^{5} \Delta w_j(\Delta MW) F_j \qquad (14)$$

where Δw_j is the mass fraction of polymer made on site type j eluting from the GPC column set in the interval ΔMW. The mass fractions Δw_j are obtained from the integration of the Flory distribution associated with each site type:

$$\Delta w_j(MW) = m_j \int_{MW}^{MW+\Delta MW} w_j(MW)\mathrm{d}MW$$

$$= m_j \left\{ \begin{array}{c} (1 + MW\hat{\tau}_j)\exp(-MW\hat{\tau}_j) \\ -[1 + (MW + \Delta MW)\hat{\tau}_j] \\ \exp[-(MW + \Delta MW)\hat{\tau}_j] \end{array} \right\} \qquad (15)$$

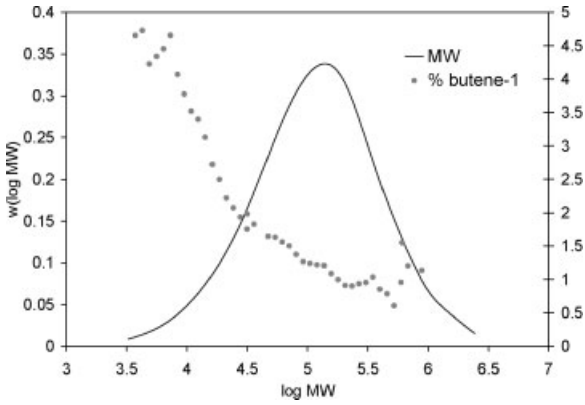

Figure 3.
GPC-IR plot of a LLDPE resin.

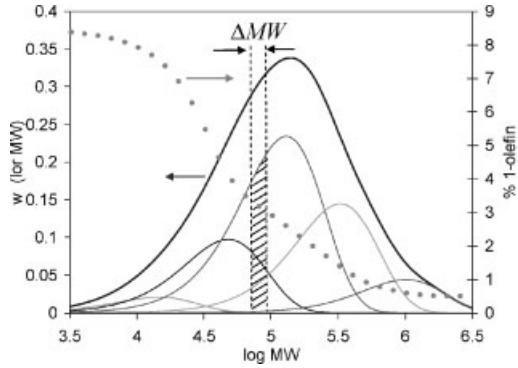

m	M_n	F
0.0382	7 000	0.09
0.18	24 000	0.04
0.433	65 000	0.03
0.2674	164 000	0.01
0.0815	510 000	0.005

Figure 4.
GPC-IR representation using five site types. The table lists the mass fractions (*m*), number average molecular weights (M_n), and 1-olefin fraction (*F*) of polymer made on each site type.

Notice that for the low molecular weight region, one may have to account for the effect of methyl end groups on the experimental IR data.

This simple representation of GPC-IR profiles permit a systematic interpretation of results observed in several academic and industrial polyolefin analytical laboratories.

Chemical Composition Distribution of Linear Chains

The bivariate distribution of chain length and chemical composition of linear polyolefins is given by Stockmayer's distribution, Equation (4). A short description of its main features is useful to clarify several properties of binary copolymers such as LLDPE and propylene/ethylene copolymers.

Figure 5 shows Stockmayer's distributions for four model single-site polyolefins with the same reactivity ratio product ($r_1 r_2 = 1$, random copolymers) and average ethylene fraction ($\overline{F} = 0.8$), but with different average chain lengths. Notice that, as the number average chain lengths of the samples increase, their distributions become narrower on the chemical composition dimension. This trend is also observed for each sample individually: shorter chains have a broader chemical composition distribution (CCD) than longer chains. This is a well known effect, caused by the statistical averaging of the chemical compositions per chain as the chains get longer. Samples with infinite length would all have comonomer fractions exactly equal to the average comonomer fraction of the polymer.

The other important property of Stockmayer's distribution is shown in Figure 6: the CCD component broadens steadily when the reactivity ratio product increases, that is, as the copolymer passes from alternating to random and, finally, to block comonomer sequences. This is also an intuitive concept, since all chains of a perfectly alternating copolymer have the same composition ($F = 0.5$), while a tendency to form long blocks of one of the comonomer will necessary increase intermolecular heterogeneity.

We can apply our Modeling Principle 1 to Stockmayer's distribution to describe the bivariate distribution of chain length (or molecular weight) and chemical composition of polyolefins made with multiple site catalysts. In this case, the following generic expression applies,

$$W(r,F) = \sum_{j=1}^{n} m_j w_j(r,F) \tag{16}$$

where $w_j(r,F)$ for each site is given by Equation (4). It should be clear that this equation can be transformed into a molecular weight distribution and expressed in either linear or log scale, using the transformations demonstrated above for Flory's distribution.

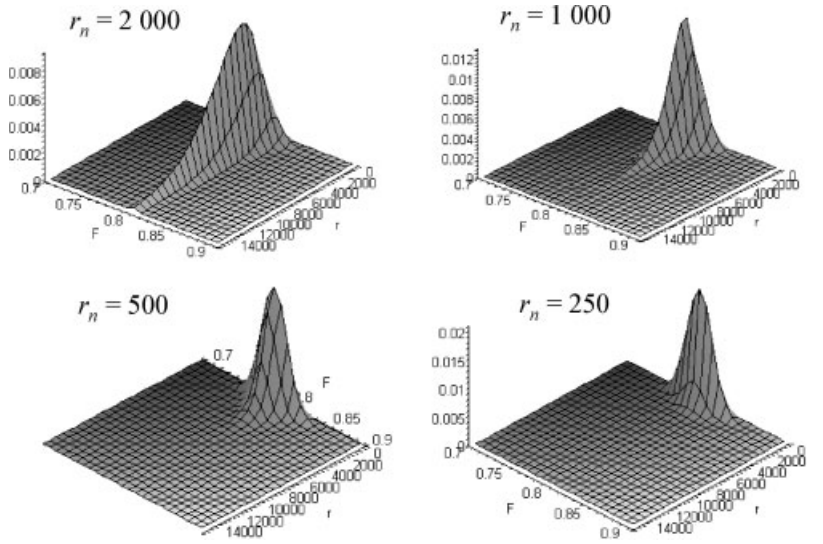

Figure 5.
CLD and CCD of four model single-site polyolefin with different number average chain lengths, r_n. Model parameters: $\bar{F} = 0.8$, $r_1 r_2 = 1$, and $\tau = 1/r_n$.

Figure 7 illustrates two bivariate distributions for LLDPE resins. The experimental distribution on the left side was measured using Polymer *Ch*ar CFC 300, a cross fractionation instrument that combines fractionation by temperature rising elution fractionation (TREF) and GPC,[8] while the distribution on the right side of the figure is a model representation using Equation (16) for a three site-type catalyst.

Very few polyolefin characterization laboratories have cross-fractionation instruments available, but most have either a TREF and/or a crystallization analysis fractionation (Crystaf) unit. We can obtain the CCD component of Stockmayer's distribution with the integration:

$$w(F) = \int_0^\infty w(r,F)\mathrm{d}r = \frac{3}{4\sqrt{2\beta\tau}\left[1+\frac{(F-\bar{F})^2}{2\beta\tau}\right]^{5/2}} \quad (17)$$

We will use Equation (17) to help us define our second modeling principle:

Principle 2: Individual microstructural distributions can be obtained from the integration of multivariate distributions.

Notice that we had already used Modeling Principle 2 to isolate the CLD component, Equation (4), from Stockmayer's distribution.

Figure 8 shows how the breadth of the CCD depends on the product of the parameters β and τ. The distribution broadens as the polymer chains become shorter (increasing τ) or the copolymer chains become blockier (increasing β). These trends had already been described in Figure 5 and 6, and appear now as part of a lumped parameter given by the product $\beta\tau$. Figure 8 captures the essence of olefin copolymer microstructure in a very elegant plot.

Similarly to the procedure we adopted to describe the MWD of polyolefins made with multiple-site catalysts, the CCD of polyolefins made with these catalysts can be represented as a weighted superposition of single-site CCDs:

$$W(F) = \sum_{j=1}^{n} m_j w_j(F) \quad (18)$$

The MWD and CCD (measured as TREF elution profiles) of an ethylene/1-butene copolymer made with a heterogeneous Ziegler-Natta catalyst is shown in

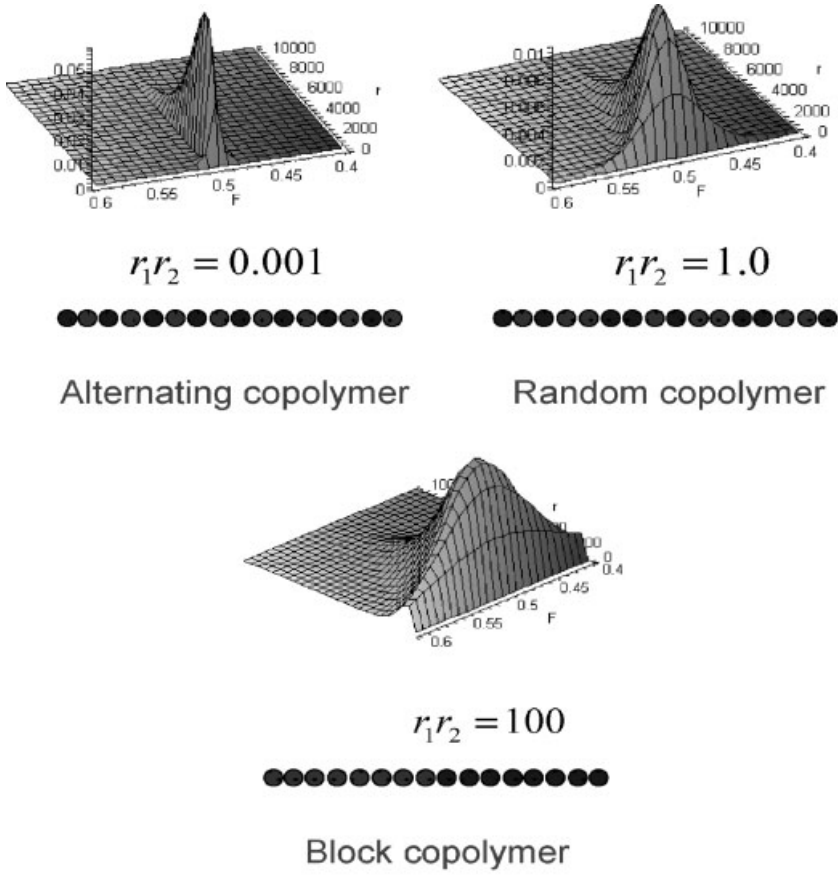

Figure 6.
CLD and CCD of three model single-site polyolefin with different reactivity ratio products, r_1r_2. Model parameters: $\overline{F} = 0.5$, $\tau = 0.001$.

Figure 9. Both profiles can be well represented with four site types. It should be noticed, however, that TREF and Crystaf profiles are related to, but are not in fact the CCD described by Equation (17). Therefore, the mathematical treatment illustrated in Figure 9 is only a first over simplified approximation. The development of fundamental models for TREF and Crystaf is a hard subject that is beyond the scope of this short review.[9,10]

Hyphenated Techniques: TREF-LS

When a light-scattering detector is added to TREF, it is possible to measure the weight average molecular weight (M_w) of polyolefin as a function of elution temperature or comonomer fraction. This technique provides a complementary analysis to the other hyphenated technique, GPC-IR, described above. Similar information can also obtained by projecting the CFC results onto the TREF elution temperature plane and computing the M_w for each elution temperature.

Figure 10 shows one analytical result for an ethylene/α-olefin copolymer with rather complex microstructure. We notice that there is a strong correlation between the elution temperature (or comonomer fraction) and the weight average molecular weigh of the polymer. The trends for the

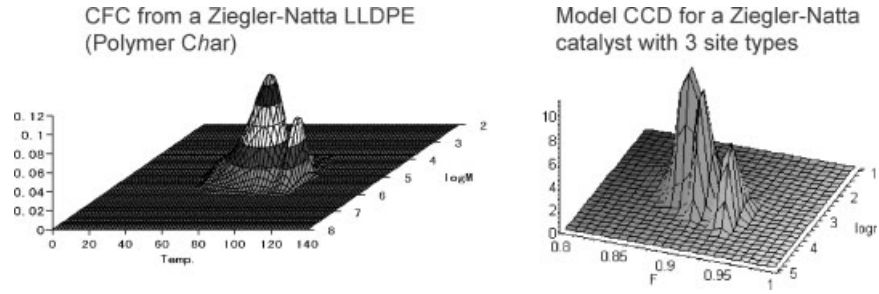

Figure 7.
Bivariate distributions for experimental (left) and model (right) LLDPE resins. The temperature axis on the experimental distribution can be converted into a comonomer fraction.

low crystallinity peak (indicated in the oval section in Figure 10) are particularly interesting: M_w passes through a maximum as we go across the peak.

Once again, the fundamental microstructural models we have been working with in this article can help us understand this trend. The weight average chain length (r_w) of a polymer as a function of its composition can be calculated from Stockmayer's distribution as:

$$r_w(F) = \int_0^\infty rw(r,F)\mathrm{d}r = \frac{15\beta^3\tau^2}{[2\beta\tau + (F-\overline{F})^2]^{7/2}} \quad (19)$$

Similarly, the number average chain length (r_n) is calculated as:

$$r_n(F) = \int_0^\infty rf(r,F)\mathrm{d}r = \frac{3\beta^2\tau}{[2\beta\tau + (F-\overline{F})^2]^{5/2}} \quad (20)$$

where $f(r,F)$ is Stockmayer's *molar* distribution:

$$f(r,F) = \frac{w(r,F)}{r\tau} \quad (21)$$

Finally, the polydispersity index as a function of chemical composition is given by:

$$PDI(F) = \frac{r_w(F)}{r_n(F)} = \frac{5\beta\tau}{2\beta\tau + (F-\overline{F})^2} \quad (22)$$

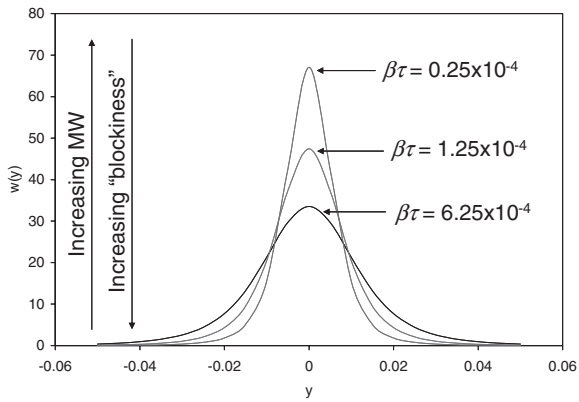

Figure 8.
CCD component of Stockmayer's distribution. The lumped parameter $\beta\tau$ determines the breadth of the CCD.

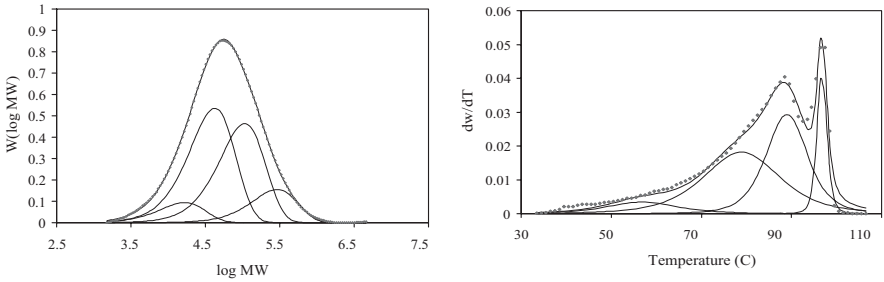

Figure 9.
MWD and CCD of a heterogeneous Ziegler-Natta ethylene/1-butene copolymer represented with four single-site populations. Model parameters: $m_1 = 0.074$, $m_2 = 0.428$, $m_3 = 0.372$, $m_4 = 0.126$; $M_{m1} = 8\,300$, $M_{n2} = 21\,000$, $M_{n3} = 53\,000$, $M_{n4} = 150\,000$; $T_1 = 57\,^{\circ}C$, $T_2 = 79\,^{\circ}C$, $T_3 = 89\,^{\circ}C$, $T_4 = 97\,^{\circ}C$. (The TREF elution temperature can be translated into 1-butene fraction with a calibration curve that accounts for the effect of 1-butene molar fraction and blockiness.)[11]

Equation (19) and (22) are shown in Figure 11, together with a CCD of a model binary copolymer. Notice that the trends predicted for r_w are the same as the ones measured for the M_w of the lowest crystallinity peak in Figure 10. This result confirms one of our previous observations with Stockmayer's distribution that the comonomer fraction in the longer chains approximates more closely the average comonomer fraction in the whole copolymer. Since the peak position in TREF is associated with the average comonomer fraction in the copolymer, we should expect that the molecular weight should increase as we get closer to this peak. Interestingly, the PDI also passes through a maximum value of $PDI = 2.5$ when $F = \overline{F}$ at the peak position for a polymer made with a single site catalyst. To our knowledge, this theoretical prediction has not been validated experimentally yet.

Our third and last modeling principle can now be defined:

Principle 3: Average properties can be obtained from a bivariate distribution by integrating over one of its dimensions.

The TREF-M_w profile for the multisite catalyst shown in Figure 10 can now be described as a superposition of CCD curves

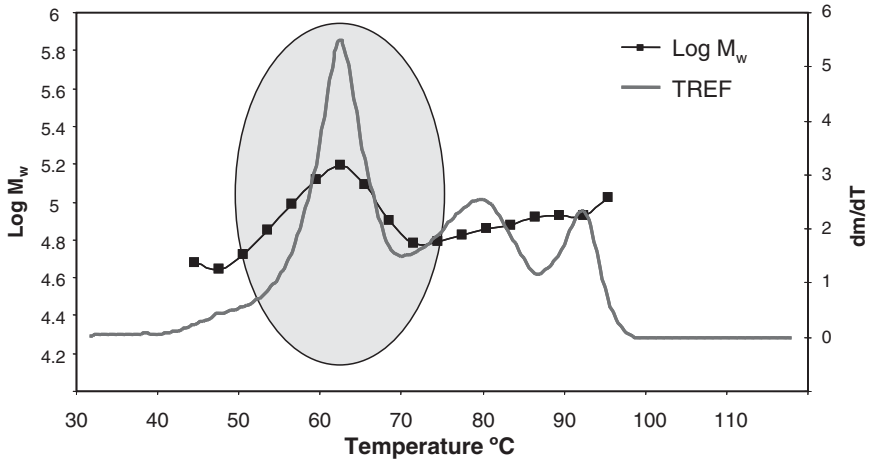

Figure 10.
TREF – M_w plot of an ethylene/α-olefin copolymer with complex microstructure (Polymer Char).

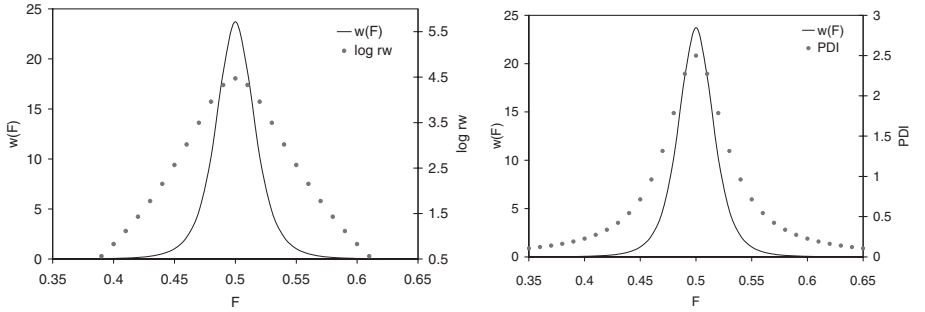

Figure 11.
Weight average chain length (r_w) and polydispersity index (*PDI*) of a binary model copolymer as a function of comonomer composition. Model parameters: $r_n = 500$, $\overline{F} = 0.5$, $r_1 r_2 = 1$.

and average weight average chain lengths (R_w) with the equation,

$$R_w(F) = \sum_{j=1}^{n} \Delta w_j(F) m_j r_{w_j}(F) \tag{23}$$

where $\Delta w_j(F)$ is the fraction of polymer with comonomer composition F made on site type j, calculated as:

$$\Delta w_j(F) = \int_{F}^{F+\Delta F} w_j(F) \mathrm{d}F \tag{24}$$

Figure 12 shows a model plot for three site types. These results are only qualitative; they represent trends, not actual values, since the representation of TREF profiles directly from Stockmayer's distributions is not accurate enough for quantitative calculations.

Long Chain Branching Distribution

Figure 13 shows the predicted distributions of chain length and comonomer composi-

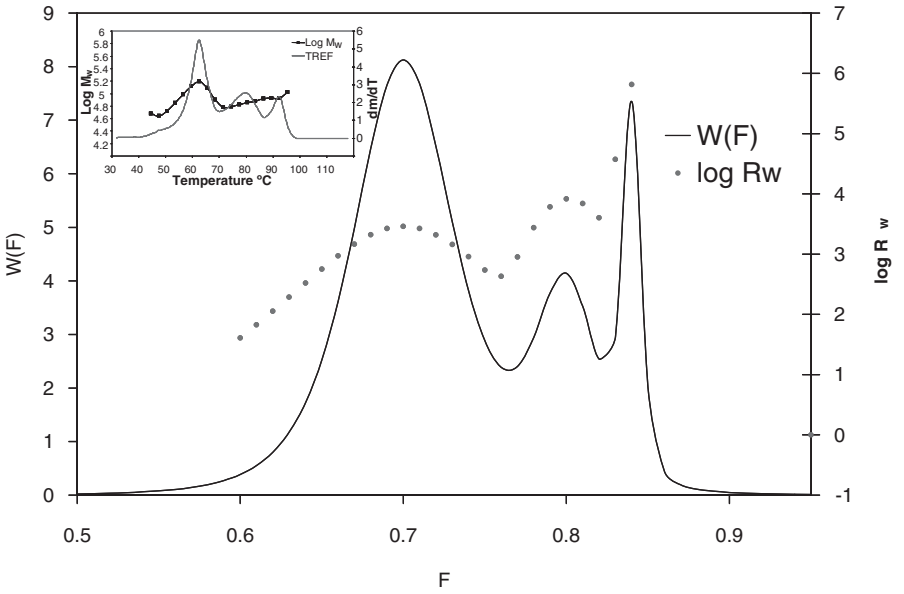

Figure 12.
CCD-R_w profile for a model three-site copolymer. The theoretical plot was adjusted to resemble the experimental plot (insert) but this representation is only qualitative.

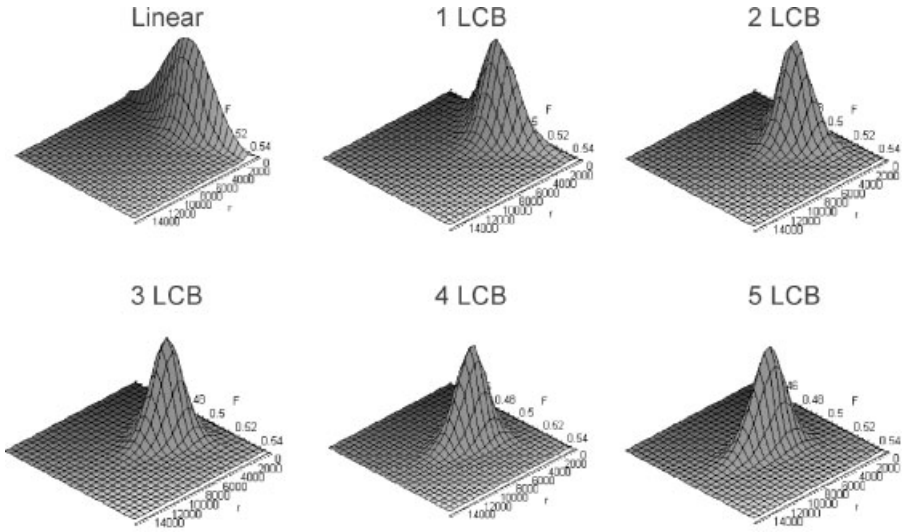

Figure 13.
Trivariate distribution of chain length, chemical composition and long chain branching. Model parameters: $\tau = 0.002$, $\overline{F} = 0.5$, $r_1 r_2 = 1$.

tion for chains with different number of LCBs per chain, as defined by Equation (1). As the number of LCBs per chain increases, the CLD move towards higher averages and the CCD becomes narrower. This equation quantifies the intuitive notion that more branched chain will have higher average lengths and that longer chains will have compositions that are closer to the average copolymer composition. This is, of course, the same prediction given by Stockmayer distribution for linear chains.

Each of the distributions shown in Figure 13 are normalized but, in reality, their fractions in the whole polymer will vary depending on the polymerization conditions.[1,2,12] Regardless of these conditions, the less branched chains always have higher molar fractions (but not necessarily higher mass fractions) than more branched chains.

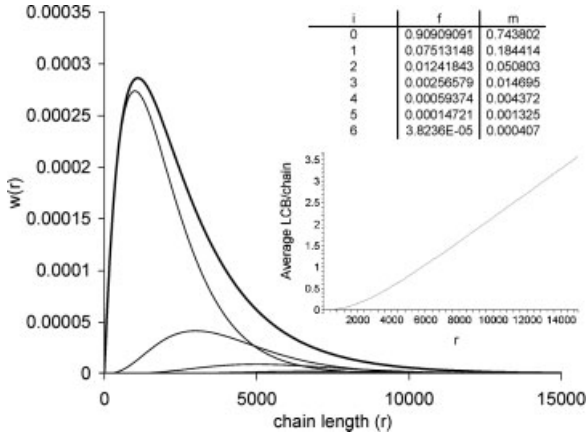

Figure 14.
CLD and average LCB/chain distributions for a model branched polymer. Model parameters: $\alpha = 0.1$ and $\tau = 0.001$.

Molar and mass fractions of populations with i LCBs per chain are given by the equations:

$$f_i = \frac{(2i)!}{i!(i+1)!}\frac{\alpha^i}{(1+\alpha)^{2i+1}} \quad (25)$$

$$m_i = \frac{(2i)!}{i!(i+1)!}\frac{\alpha^i(1-\alpha)(2i+1)}{(1+\alpha)^{2i+2}} \quad (26)$$

The parameter α is a function of polymerization conditions and catalyst type and varies from zero (no LCB formation) to one (infinity LCB formation).[12]

Figure 14 shows the overall and individual CLDs of a model branched polymer. The average number of LCBs as a function of chain length is also illustrated. Notice that most of the polymer chains are linear, but a significant fraction contain LCBs.

It is also interesting to notice how the average number of LCBs per chain increases with chain length. An analytical solution for this distribution is possible, but too lengthy to show here. The final expression is given below:

$$\overline{LCB} = \frac{\phi I_2(2\phi)}{I_1(\phi)} \quad (27)$$

$$\phi = \frac{r\tau\sqrt{\alpha}}{1+\alpha} \quad (28)$$

and I_k are modified Bessel functions of first kind and order k.

Conclusions

In this article we provided an overview of equations that are useful to interpret microstructural distributions of polyolefins. Simple expressions for the distributions of chain length, chemical composition and long chain branching can be found for polymers made with single site catalysts. The treatment of polyolefins made with multiple site catalysts is more elaborate and there is no consensus in the literature on how to best model their microstructure. A simple approach consists in assuming that multiple site catalysts behave as a collection of single site catalysts, but this approach is used for convenience only and is still subject to experimental scrutiny.

We have also shown that these distributions capture the essence of different microstructural characterization analytical approaches, from techniques using single to dual detectors (hyphenated-techniques) and more sophisticated cross-fractionation analyses.

[1] J. B. P. Soares, A. E. Hamielec, *Macromol. Theory Simul.* **1996**, *5*, 547.
[2] J. B. P. Soares, A. E. Hamielec, *Macromol. Theory Simul.* **1997**, *6*, 591.
[3] W. H. Stockmayer, *J. Chem. Phys.* **1945**, *13*, 199.
[4] P. J. Flory, *J. Am. Chem. Soc.* **1936**, *58*, 1877.
[5] Z. Schulz, *Physik. Chem.* **1937**, *B30*, 184.
[6] J. D. Kim, J. B. P. Soares, G. L. Rempel, *J. Polym. Sci.: Part A: Polym. Chem.* **1999**, *37*, 331.
[7] J. B. P. Soares, A. E. Hamielec, *Polymer* **1995**, *36*, 2257.
[8] B. Monrabal, et al., *Macromol. Symp.* this issue.
[9] J. B. P. Soares, S. Anatawaraskul, *J. Polym. Sci.: Part B: Polym. Chem.* **2005**, *43*, 1557.
[10] S. Anantawaraskul, J. B. P. Soares, P. M. Wood-Adams, *Adv. Polym. Sci.* **2005**, *182*, 1.
[11] A. A. da Silva Filho, G. B. de Galland, J. B. P. Soares, *Macromol. Chem. Phys.* **2000**, *201*, 1226.
[12] J. B. P. Soares, *Macromol. Mater. Eng.* **2004**, *289*, 70.

